Progress In Electromagnetics Research Letters, Vol. 98, 85–94, 2021

Design of Low-Profile and Safe Low SAR Tri-Band Textile EBG-Based Antenna for IoT Applications

Wissem El May[1, 2], Imen Sfar[2], Jean M. Ribero[1], and Lotfi Osman[2, *]

Abstract—A coplanar tri-band wearable antenna combined with an electromagnetic bandgap (EBG) structure is described for sub-6 GHz 5G and wireless local area network (WLAN) applications. The proposed antenna is fully implemented in textile materials thus offering a robust, compact, and discreet solution to meet the requirements of wearable applications. The addition of the EBG structure increases the textile antenna performance in terms of radiation patterns in the presence of the human body. The experimental results show that the proposed design exhibits tolerance to various bending conditions as well as loading by body tissues. In addition, to ensure the safety of the design for human health, the values of the specific absorption rate (SAR) have been reduced by more than 95%, which complies with the international standard. This design could thus be considered as a good candidate for IoT applications compared to the current state of the art while having a tri-band behavior and smaller volume.

1. INTRODUCTION

With the emergence of advanced technologies of Internet-of-Things in many fields, the investigation and development of Body-Centric applications including military mobile computing, health monitoring, sports, and tracking have been growing rapidly. Consequently, investigating wearable antennas with compact size, flexibility, and comfortable embedding to the body or into clothing covering the bands of these applications is in urgent need [1]. Most of the proposed flexible wearable antennas are based on polymers [2], textiles [3, 4], or flexible ceramics [5]. Among flexible materials, textiles are the most widely employed materials for wearable antennas due to their ease of integration on the clothes compared to a traditional design.

However, the main goal when wearable textile antennas are designed is their ability to provide multi-band operation with compact size, high gain, broad radiation efficiency, and minimizing the interaction between antenna and human body [6], even though they are located close to each other. In literature, a diverse range of techniques have been reported for performance enhancement of the antenna and reducing interaction between the antenna and human tissue characterized by specific absorption rate (SAR). One popular technique is the utilization of antennas incorporating metamaterial such as electromagnetic bandgap [7, 8]. Electromagnetic Bandgap (EBG) is widely used in antenna designs to suppress surface waves and generate a zero-degree phase, which improves the gain and reduces the effects of the proximity of the human body on the antenna.

In the literature, several finite-sized EBGs with single and dual-band behavior for wireless local area network (WLAN) applications [9-11] have improved antenna performance only in the desired operating frequency bands. Consequently, the required gap between the antenna and reflector greatly affects the impedance matching for all of the designed frequency bands. Furthermore, most of the proposed

Received 11 May 2021, Accepted 11 June 2021, Scheduled 21 June 2021

* Corresponding author: Lotfi Osman (lotfi.osman@supcom.tn).

[1] LEAT, Department of Electronics, University Nice Sophia Antipolis, 06903, France. [2] Microwave Electronics Research Laboratory, LR18ES43, Department of Physics, Faculty of Sciences of Tunis, University of Tunis El Manar, 2092, Tunisia.

antenna designs suffer from a relatively large size or high profile and do not meet the requirements presented to date.

In this work, we propose a low profile purely textile antenna loaded by an EBG structure with multiband characteristic, high gain, and good isolation while achieving low SAR level, which is one of the first studies to propose an antenna fully textile for IoT applications.

The proposed antenna covers the WLAN (2.45/5.8 GHz) and sub-6-GHz 5G (3.50 GHz) applications [12] providing multiple services using a single structure, which has not been covered in the existing literature. The antenna and EBG were modeled and simulated under CST MWS Software, and measurements were carried out to validate the results. The organization of the communication is as follows. The design and characterization of the antenna and EBG structure are first presented in Section 2. In Section 3, the analysis of the antenna on the EBG plane is discussed to evaluate the overall integrated design. Finally, Section 3 examines the on-body performance of the antenna, structural bending, and SAR.

2. ANTENNA DESIGN

2.1. Geometry of the Proposed Antenna

The geometry of the proposed multiband antenna is illustrated in Figure 1(a) which consists of a substrate layer made of wool felt with a thickness of 1 mm, relative permittivity of 1.2, and loss tangent angle of 0.02, which are characterized by the microstrip T-resonator method [13]. A Laser Cutting Machine (VEVOR) is used to cut the conductive layer made from Shieldit Super material with a thickness of 0.17 mm. The monopole antenna structure is a coplanar design consisting of a rectangular patch and dual meander strips, surrounded by the normal ground of a coplanar waveguide (CPW) line. The antenna size is $45.3 \times 34.1\,\text{mm}^2$, and detailed dimensions are given in Table 1.

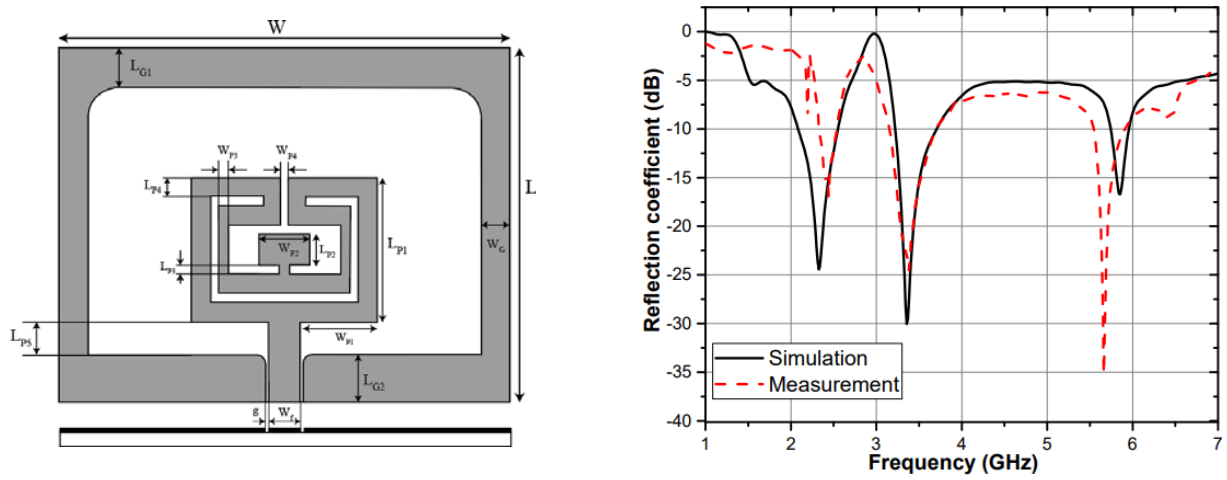

(a) (b)

Figure 1. (a) Geometry of the proposed textile antenna. (b) Reflection coefficient (S_{11}) of the antenna.

The simulated return loss of the tri-band textile antenna is compared with the measured one in Figure 1(b). It can be observed that the frequency antenna achieves impedance bandwidths of 10% (2.31–2.55 GHz) and 7% (5.53–5.94 GHz) covering the Wi-Fi bands, whereas the measured bandwidth at sub-6 GHz 5G band is 16% (3.13–3.70 GHz). It shows that the measured results have discrepancies compared to the predicted one, which may be due to imperfections reproduced during the fabrication process (dimensional uncertainty). Simulations show the current excitation at the three selected frequency bands 2.45, 3.5, and 5.8 GHz which are depicted in Figure 2. It is observed that at the lower resonance 2.45 GHz, the currents mainly distribute on the higher parts of the CPW feed line and in the outer strips. Similarly, at 3.5 GHz, the currents are primarily allocated at the meander strips

Table 1. Dimensions of the proposed antenna and EBG unit cell.

Parameter	Value (mm)	Parameter	Value (mm)	Parameter	Value (mm)
W	45.3	L_{p4}	2	L_e	40.6
L	34.1	L_{p5}	3.4	L_{e1}	37
L_{G1}	3.75	W_{p1}	8.13	L_{e2}	4
L_{G2}	3.4	W_{p2}	5.38	L_{e3}	11
W_G	3.2	W_{p3}	1	L_{e4}	10
L_{p1}	15.1	W_{p4}	0.8	W_e	28
L_{p2}	3.24	W_f	3.2	W_{e1}	1.5
L_{p3}	1	g	0.2	W_{e2}	1.2

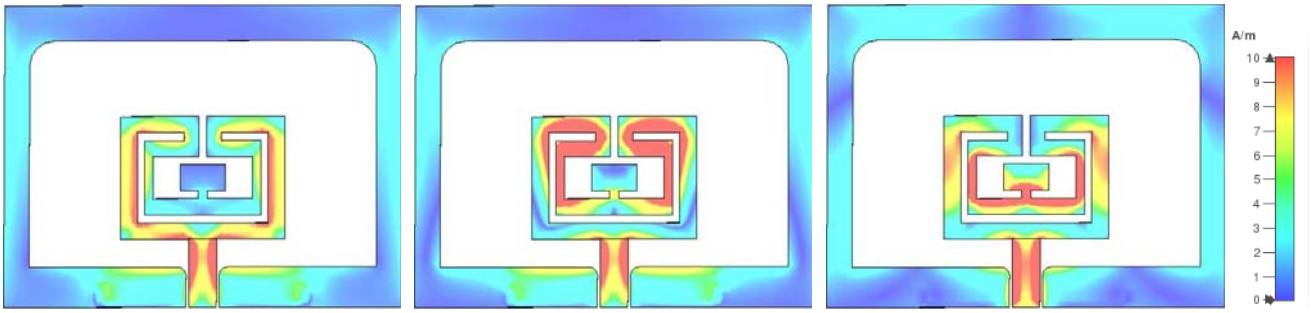

(a) (b) (c)

Figure 2. Surface current distribution of the CPW antenna. (a) 2.45 GHz, (b) 3.5 GHz, (c) 5.8 GHz.

of the antenna, while the inner patch and strips fundamentally resonate in the upper-frequency band 5.8 GHz. The radiation patterns of the antenna are omnidirectional which are described later, and the gains of the latter are 2.88, 3.53, and 4.01 dBi at 2.45, 3.5, and 5.8 GHz, respectively.

For the proposed antenna, the main beams are directed towards the front and rear, thus inducing a more intense absorption of power inside the human body. To overcome this, an Electromagnetic Bandgap (EBG) structure with multi-band behavior can be used as an antenna reflector to reduce the human body's exposure to the radiation plane and obtain a more compact textile antenna by favoring their directivities.

2.2. Design of the Triple Band EBG Structure

The geometry of the EBG unit cell is inspired from [14] and depicted in Figure 3(a). The design is based on a simple rectangular patch structure before the introduction of a rectangular slot in the patch. Next, four perpendicular rectangular stubs in the patch are added to create various metallic sectors responsible for multi-band characteristics. The optimized parameters of the unit cell are also listed in Table 1.

Diverse methods were investigated to characterize the EBG materials at the demand frequency such as the suspended transmission line method [15, 16]. For the proposed technique, the EBG array is placed between the microstrip transmission line and ground, connecting with two 50 Ω SMA connectors and excited such that one port was acted as a source and the other as a matched load. The EBGs are generally considered to be a high impedance periodic structure (HIS) that can stop the propagation of surface waves in certain frequency ranges and acts as an artificial magnetic conductor (AMC) when it creates zero phase reflection [17]. An optimum EBG array consisting of 2×2 elements is chosen and

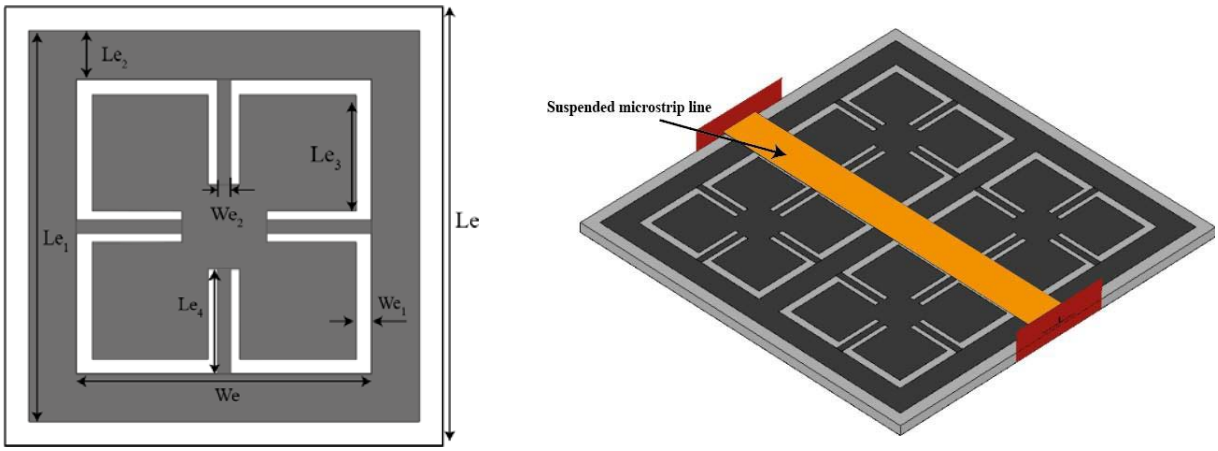

Figure 3. Proposed EBG surface: (a) Geometry of one cell; (b) Suspended microstrip line method of EBG array.

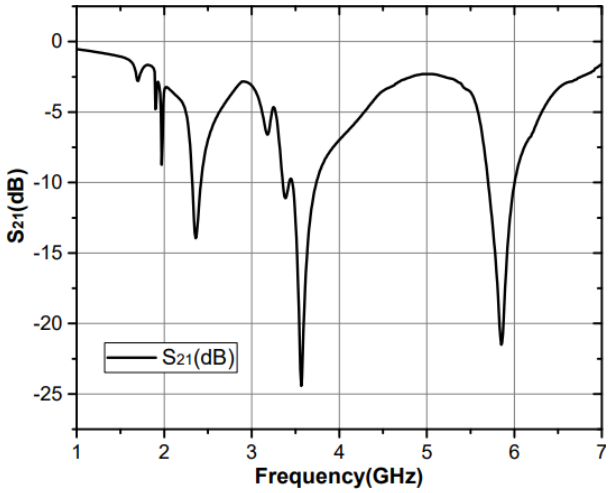

Figure 4. Simulated S_{21} bandgap response EBG using a suspended line method.

computed by using CST Microwave Studio placed on a felt textile material with overall dimensions of $69 \times 69 \times 2\,\text{mm}^3$ depicted in Figure 3(b). From the simulated transmission coefficient (S_{21}) less than 10 dB as can be viewed in Figure 4, it can be seen that the proposed EBG array has three stopbands at 2.4, 3.5, and 5.8 GHz.

3. INTEGRATION OF THE CPW TEXTILE ANTENNA AND EBG STRUCTURE

In this section, the textile CPW antenna is placed above the EBG array using a thin 2 mm foam layer as a separation between them to reduce any mismatch and short circuits, which leads to good results in terms of the reflection coefficient. The integrated design is presented in Figure 5(a).

The measured and simulated (S_{11}) of the textile antenna with and without EBG in free space are plotted in Figure 5(b). It demonstrates that the (S_{11}) is reasonably stable and covers useful frequency bands needed for wireless systems and IoT applications. Comparing the (S_{11}) of the antenna without EBG and the complete antenna/EBG combination, we observe some parasitic frequencies with a slight shift at the high-frequency band when the EBG is incorporated. This may be caused by the deviations of the testing environment and the manufacturing tolerances of the model [7, 10, 18].

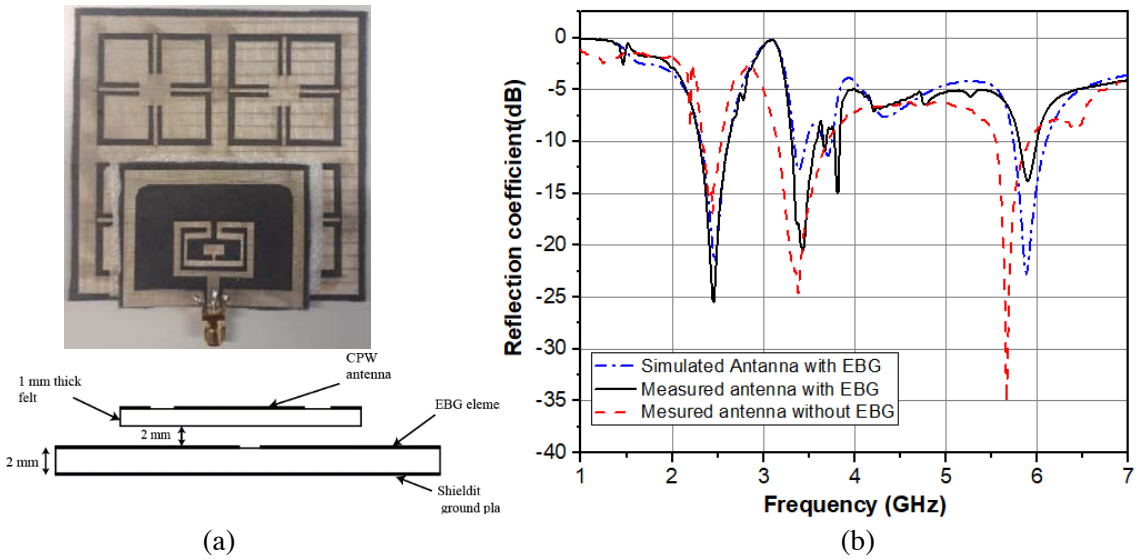

Figure 5. (a) Configuration of the antenna with EBG structure. (b) Measured and simulated (S_{11}).

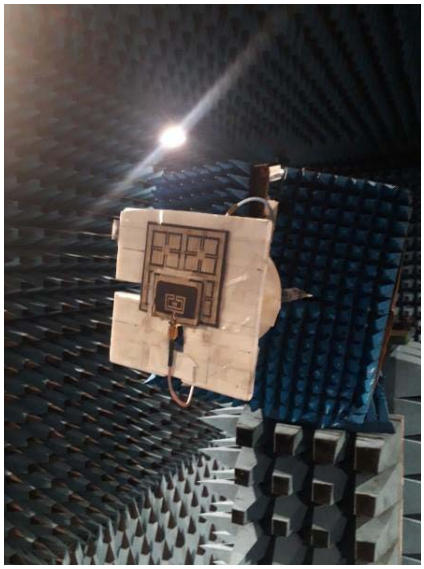

Figure 6. Measured EBG antenna in an anechoic chamber.

The measurement of the radiation patterns of the antenna with and without the EBG backing in H-plane and E-plane at 2.4, 3.5, and 5.8 GHz obtained in a Stargate anechoic chamber is illustrated in Figure 6. It is shown in Figure 7 that the antenna alone at each frequency band has an omnidirectional pattern in the H-plane and identical to that of a monopole antenna in the free space in the E-plane. In other words, the antenna having radiation in the negative and positive z-axis indicates significant backward radiation. However, the presence of the EBG reflector leads to more significant radiation for z positive and decreases the back radiation toward the human tissues. The measured gain increases from 5.11, 6.43, and 7.41 dBi at 2.45, 3.5, and 5.8 GHz, respectively, as compared to 2.88, 3.53, and 4.01 dBi of the antenna without EBG.

4. ANTENNA ON HUMAN BODY

4.1. Bending Evaluation

In mobile systems, wearable antennas are intended to be in some cases deformed or conformed to human body surfaces during operation especially when they are made of flexible textile. The impact of

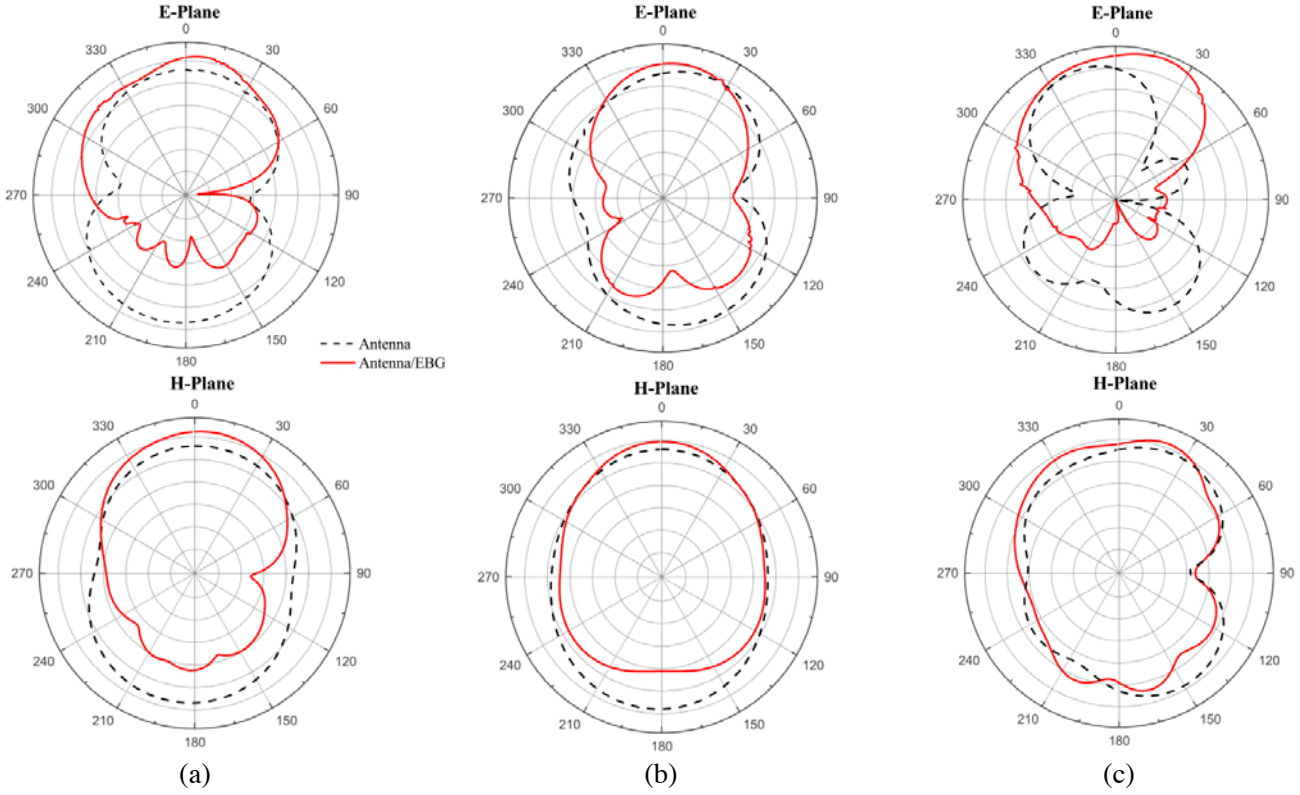

Figure 7. Measured E- and H-plane radiation patterns with and without EBG: (a) 2.45 GHz, (b) 3.5 GHz, (c) 5.8 GHz.

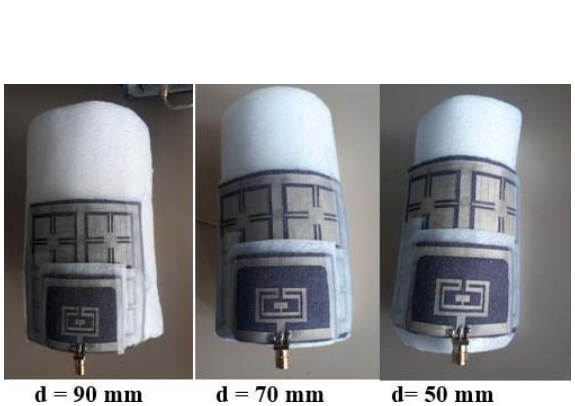

(a)

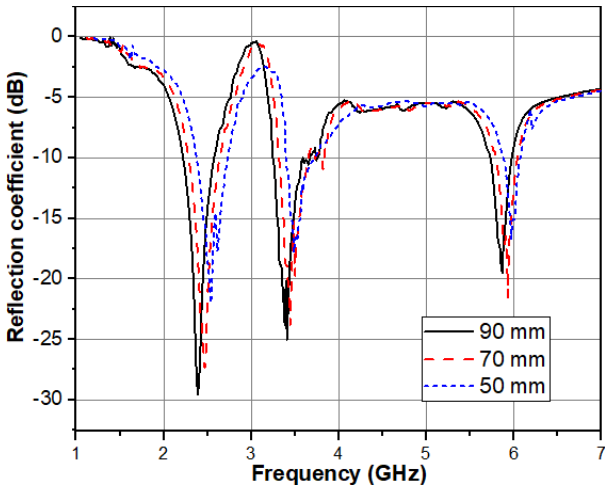

(b)

Figure 8. (a) Photographs of the antenna under three bending conditions. (b) Reflection coefficient (S_{11}).

curvatures on the antenna performance was experimentally validated with several degrees of bending to ensure its consistency before the antenna is loaded onto a human body curvature. This is done by positioning the antenna on a foam cylinder with different diameters, namely 90, 70, and 50 mm as illustrated in Figure 8(a). The measured (S_{11}) response of the three scenarios is depicted in Figure 8(b). It can be observed that the impedance bandwidth of the resonance frequencies is slightly shifted compared to that in the flat condition. Overall, the results exhibit the robustness of the adaptation of the total structural even under various curvature conditions.

4.2. Human Tissues Loading Evaluation

The next investigation of the proposed antenna with EBGs is to evaluate its performance when the antenna is loaded onto the human body. The antenna is located directly on different parts of a real male volunteer (Chest, Arm, and Leg) as seen in Figure 9(a). The comparison results of the measured reflection coefficient (S_{11}) are presented in Figure 9(b). It shows that the proposed antenna still resonates at the operating frequencies including 2.45/3.5/5.8 GHz for the case when the proposed antenna was positioned above the body despite the high dielectric nature of human tissue. A slight difference between the curves was observed, and the bandwidths of (S_{11}) < -10 dB cover the desired bands in all conditions.

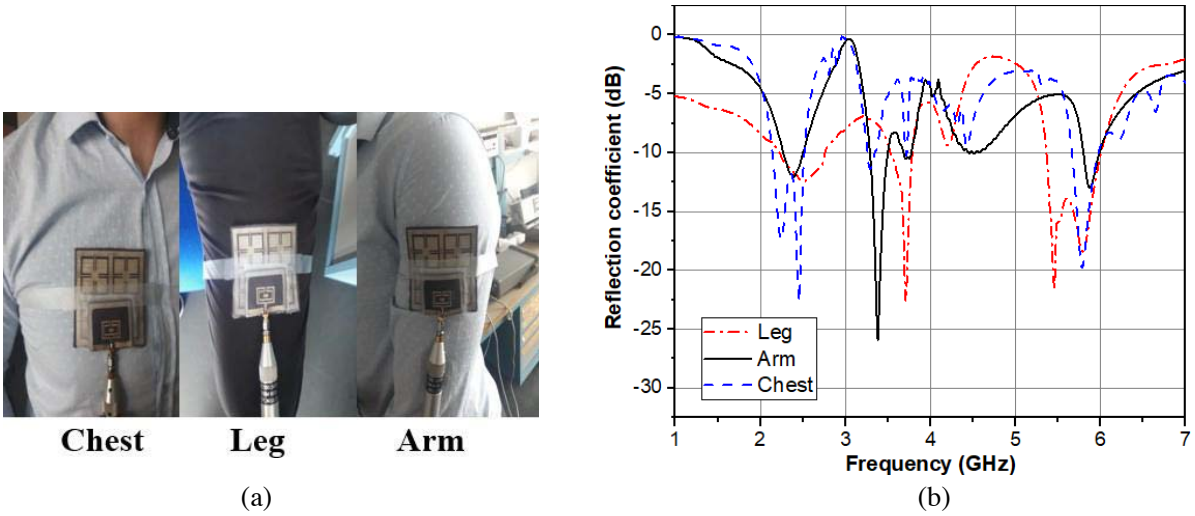

Figure 9. Measured (S_{11}) of the proposed antenna placed on human tissue. (a) Antenna performance evaluation at chest, legs, and arm. (b) Measured reflection coefficient (S_{11}).

4.3. Specific Absorption Rate

To justify the ability of the proposed design to exploit as a wearable antenna without affecting the human tissue, the maximum Specific Absorption Rate (SAR) value of the antenna with/without EBG was carried out using CST MWS software and expressed as follows [19]:

$$\mathrm{SAR} = \sigma \frac{|E|^2}{\rho} \tag{1}$$

where ρ is the volume density of the human tissues, σ the conductivity, and E the electric field. The SAR of the prototype is analyzed using a multilayer rectangular human tissue health model. The thickness and dielectric properties of each layer (Skin, Fat, and Muscle) considered in the body model are taken from [20] and tabulated in Table 2. The size of the model was $120 \times 120 \times 46\,\mathrm{mm}^3$, and the distance between the model and the prototype was 1 mm. The simulations of the SAR results are presented in Table 3, and the input source power for SAR calculations in this work is set at 0.5 W (rms) using the IEEE C95.3 for an average of more than 10 g of tissue volume. Thanks to the presence of the EBG

Table 2. Permittivity, loss tangent, density, and thickness of the 3 layered rectangular body model.

	Dielectric constant	Loss tangent	Density (kg/m^3)	Thickness (mm)
Skin (Wet)	49.9	0.60	1100	1
Fat	5.58	0.33	900	5
Muscle	57.13	0.63	1040	40

Table 3. Simulated SAR of the proposed antenna for 10 g of tissue.

Frequency (GHz)	Antenna without EBG	Antenna with EBG
2.45	12.98	0.471
3.5	8.75	0.860
5.8	19.87	0.146

structure as a reflector, the SAR values are attenuated more than 91.5% at the three selected frequency bands, which are less than the safe level for the European standard 2 W/kg. Figure 10 reveals the three-dimensional SAR of the antenna with EBG at 1 mm away from the biological model.

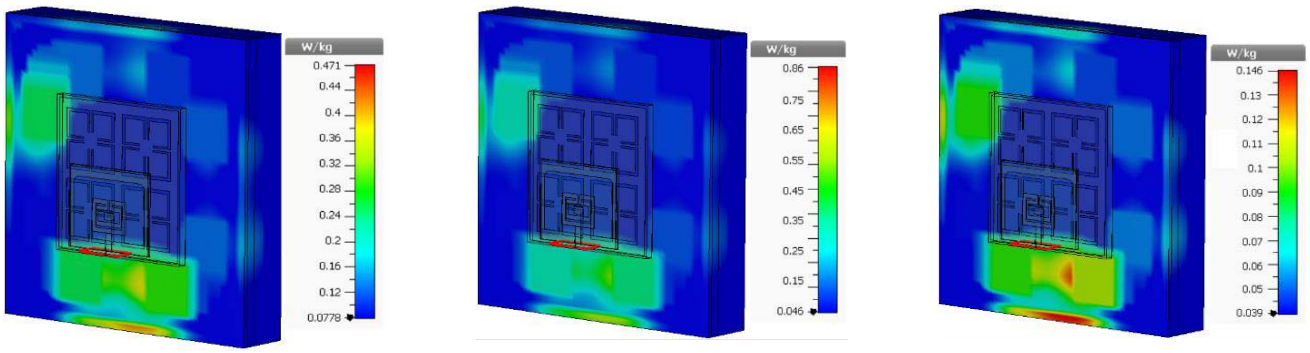

(a) (b) (c)

Figure 10. SAR levels at 1 mm far from the skin: (a) 2.4 GHz, (b) 3.5 GHz, (c) 5.8 GHz.

A comparison of the performance of the proposed textile EBG-antenna with similar studies is presented in Table 4, which indicates that the solution proposed owns the advantages of high gain, smaller size, and gives tri-band characteristics compared to the structures in similar studies.

Table 4. Comparison of the proposed antenna with some references.

Reference number	Operating Band (GHz)	Size (mm^3)	Gain (dBi)	Bandwidth (%)	SAR (W/kg)
[7]	2.4/5.8	$120 \times 120 \times 4$	6.4/7.6	4/16	0.043/0.12
[9]	2.45	$81 \times 81 \times 4$	7.3	14.7	0.23
[10]	1.8/2.45	$150 \times 150 \times 4$	-	10/5.08	0.024/0.016
[11]	2.4/5.5	$85 \times 85 \times 5$	-	12/10	-
[Our work]	2.4/3.5/5.8	$69 \times 69 \times 5$	5.11/6.43/7.41	10/16/7	0.47/0.86/0.14

5. CONCLUSION

A robust, conformal wearable CPW antenna over a 2×2 EBG array with triple-band performance covering the Wi-Fi band (2.45/5.8 GHz) and sub-6 GHz 5G band (3.5 GHz) has been developed and produced. The incorporated design is made entirely from textile materials and is highly conformable so that it can be integrated into our everyday clothes. The EBG greatly increases the gain of the CPW antenna, which reduces the back radiation to the body. Bending measurements on the human body have been carried out and have given satisfactory results. In addition, the calculated SAR values of the prototype were reduced by more than 91% in the presence of EBG. As a result, the prototype can be seen as a very promising solution for IoT applications thanks to its ability to generate a triple-band performance, simple geometry, high gain, and compact size.

REFERENCES

1. Hertleer, C., H. Rogier, L. Vallozzi, and L. van Langenhove, "A textile antenna for off-body communication integrated into protective clothing for fire fighters," *IEEE Trans. Antennas Propag.*, Vol. 57, 919–925, 2009.
2. Song, Y., D. Le Goff, G. Riondet, and K. Mouthaan, "Polymer-based 4.2 GHz patch antenna," *Proceedings of the 2020 International Workshop on Antenna Technology*, 25–28, Feb. 2020.
3. Ashyap, A. Y. I., et al., "Inverted E-shaped wearable textile antenna for medical applications," *IEEE Access*, Vol. 6, 35214–35222, 2018.
4. Atanasova, G. L. and N. T. Atanasov, "Impact of electromagnetic properties of textile materials on performance of a low-profile wearable antenna backed by a reflector," *International Workshop on Antenna Technology*, 1–4, iWAT, 2020.
5. Fang, R., R. Song, X. Zhao, Z. Wang, W. Qian, and D. He, "Compact and low-profile UWB antenna based on graphene-assembled films for wearable applications," *Sensors*, Vol. 20, 2552, 2020.
6. Gao, G.-P., C. Yang, B. Hu, R.-F. Zhang, and S.-F. Wang, "A wide bandwidth wearable all-textile PIFA with dual resonance modes for 5 GHz WLAN applications," *IEEE Trans. Antennas Propag.*, Vol. 67, No. 6, 4206–4211, Jun. 2019.
7. Zhu, S. and R. Langley, "Dual-band wearable textile antenna on an EBG substrate," *IEEE Trans. Antennas Propag.*, Vol. 57, No. 4, 926–935, Apr. 2009.
8. Yan, S., P. J. Soh, and G. A. E. Vandenbosch, "Low-profile dual-band textile antenna with artificial magnetic conductor plane," *IEEE Trans. Antennas Propag.*, Vol. 62, No. 12, 6487–6490, 2014.
9. Gao, G. P., B. Hu, S. F. Wang, and C. Yang, "Wearable circular ring slot antenna with EBG structure for wireless bodyarea network," *IEEE Antennas and Wireless Propagation Letters*, Vol. 17, 434–437, 2018.
10. Velan, S. and E. F. Sundarsingh, "Dual-band EBG integrated monopole antenna deploying fractal geometry for wearable applications," *IEEE Antennas and Wireless Propagation Letters*, Vol. 14, 249–252, 2015.
11. Mantash, M., A. C. Tarot, and K. Mahdjoubi, "Design methodology for wearable antenna on artificial magnetic conductor using stretch conductive fabric," *IETJ Mag.*, Vol. 52, 95–96, 2016.
12. Desai, A., T. Upadhyaya, J. Patel, and R. Patel, "Flexible CPW fed transparent antenna for WLAN and sub-6 GHz 5G applications," *Microw. Opt. Technol. Lett.*, Vol. 62, 2090–2103, 2020.
13. Zahedi, A., F. A. Boroumand, and H. Aliakbarian, "Analytical transmission line model for complex dielectric constant measurement of thin substrates using T-resonator method," *IET Microw. Antennas Propag.*, Vol. 14, 2027–2034, 2020.
14. Foroozesh, A. and L. Shafai, "Investigation into the application of artificial magnetic conductors to bandwidth broadening, gain enhancement and beam shaping of low profile and conventional monopole antennas," *IEEE Trans. Antennas Propag.*, Vol. 59, No. 1, 4–20, Jan. 2011.
15. Li, Y., M. Fan, F. Chen, J. She, and Z. Feng, "A novel compact electromagnetic-bandgap (EBG) structure and its applications for microwave circuits," *IEEE Transactions on Microwave Theory and Techniques*, Vol. 53, 183–190, 2005.

16. EL May. W, I. Sfar, L. Osman, and J. M. Ribero, "A textile EBG-based antenna for future 5G-IoT millimeter-wave applications," *Electronics*, Vol. 10, Jan. 2021.
17. Liu, X. Y., Y. H. Di, H. Liu, Z. T. Wu, and M. M. Tentzeris, "A planar Windmill-like broadband antenna equipped with artificial magnetic conductor for off-body communications," *IEEE Antennas and Wireless Propagation Letters*, Vol. 15, 64–67, 2016.
18. Jamaluddin, M. H., et al., "An overview of electromagnetic band-gap integrated wearable antennas," *IEEE Access*, Vol. 8, 7641–7658, 2020.
19. Hirata, A., K. Shirai, and O. Fujiwara, "On averaging mass of SAR correlating with temperature elevation due to a dipole antenna," *Progress In Electromagnetics Research*, Vol. 84, 221–237, 2008.
20. Klemm, M. and G. Troester, "EM energy absorption in the human body tissues due to UWB antennas," *Progress In Electromagnetics Research*, Vol. 62, 261–280, 2006.